

## NUMERICAL STABILITY ANALYSIS OF A PRESSURE SPACE WITH EMBEDDED DISCONTINUITIES

Fabricio S. Sousa<sup>a</sup>, Roberto F. Ausas<sup>b</sup> and Gustavo C. Buscaglia<sup>a</sup>

<sup>a</sup>*Instituto de Ciências Matemáticas e de Computação, Univ. de São Paulo, São Carlos, Brasil,  
fsimeoni@icmc.usp.br, gustavo.buscaglia@icmc.usp.br*

<sup>b</sup>*Grupo de Mecánica Computacional, Centro Atómico Bariloche e Instituto Balseiro, Av. Bustillo 9500,  
Bariloche, Argentina, rfausas@gmail.com*

**Keywords:** Finite elements, interface, discontinuous pressure, surface tension, LBB condition, Stabilization

### Abstract.

A finite element space with embedded discontinuities has been recently introduced by the authors (R. Ausas et al, *Comp. Meth. Appl. Mech. Engrg.*, 199:1019-1031, 2009; see also *Mecánica Computacional* 28:1131-1148, 2009). This space has the same unknowns as the linear, continuous finite element space, but is locally modified to accommodate discontinuities at an arbitrary interface, not coincident with the element boundaries. The motivation comes from Eulerian treatment of surface tension problems, in which there is a pressure jump at the interface. It has been shown both numerically and theoretically (G. Buscaglia and A. Agouzal, *CILAMCE*, 2009) that this space has good interpolation properties. Numerical examples have also shown that, when used as pressure space in a finite element formulation of the Navier-Stokes equations, the proposed space leads to accurate results. This suggests that inf-sup stability conditions are satisfied, but they are very hard to prove because the space depends on the (arbitrary) location of the interface. In this paper we briefly review the eigenproblems associated with the discrete inf-sup condition (D. Malkus, *Int. J. Engng. Sci.*, 19:1299-1310, 1981) and use them to numerically assess the stability and convergence of the proposed space, considering both mixed (mini-element) and stabilized (equal-order) formulations.

## 1 INTRODUCTION

One of the great challenges in an accurate and robust numerical simulation of two phase flows in the presence of surface tension effects and/or singular forces in finite-element-based computational fluid mechanics is the interpolation of variables, such as the pressure, which exhibit discontinuities at immersed interfaces not conforming with the mesh (i.e. not coincident with the element boundaries). In the last years, this has been addressed in several ways: on the one hand, in [Gross and Reusken \(2007b,a\)](#) (see also [Reusken \(2008\)](#)), the authors adopt an XFEM ([Belytschko et al., 2001](#)) enrichment of the pressure space, incorporating functions that are discontinuous at  $\Gamma$ , as had also been proposed by [Minev et al. \(2003\)](#). The main drawback of these formulations is the introduction of new unknowns that depend on the location of the interface thus requiring to rebuild the linear system structure corresponding to each interface location. An additional drawback is that the resulting linear systems are ill-conditioned. On the other hand, in two recent articles ([Ausas et al., 2010](#); [Sousa et al., 2009](#)) the authors have introduced a novel pressure space which accommodates discontinuities at a (given) interface  $\Gamma$ , which is approximated by piecewise-linear segments in 2D and piecewise-planar facets in 3D. The proposed space is nothing but the classical conforming  $P_1$  space, locally modified at those elements of the finite element partition that are cut by the interface. The modification is local, computed element-by-element, and it does not introduce any additional degrees of freedom. It is thus very easy to incorporate the proposed space into existing finite element codes. In the aforementioned articles, we have implemented the new pressure space with the two following finite element discretizations:

- i The stable  $P_1^+/P_1$  mini–element discretization
- ii The stabilized equal–order  $P_1/P_1$  discretization.

In [Buscaglia and Agouzal \(2009\)](#) it has been shown that the interpolation accuracy of the new space is  $\mathcal{O}(h^{\frac{3}{2}})$  in the  $L^2(\Omega)$ –norm, however, it remains to evaluate the stability for these two discretizations to be convergent. In the standard case without embedded discontinuities stability of these two finite element discretizations are well known (see for instance [Arnold et al. \(1984\)](#) for the  $P_1^+/P_1$  mini–element and [Hughes et al. \(1986\)](#); [Franca and Hughes \(1988\)](#) for the stabilized  $P_1/P_1$  discretization). For the  $P_1^+/P_1$  mini–element, the famous LBB condition, which guarantees well–posedness and good convergence properties of the discrete formulation is satisfied. The stabilized equal–order  $P_1/P_1$  discretization, though not satisfying the LBB condition, is rendered convergent by introducing into the variational formulation consistent elementwise stabilization (i.e. a stabilization weighted with the residue of the discrete differential operator). However, it is not immediate whether these two discretizations will remain stable with the introduced modifications by the new pressure space, even with these modifications just being active in those elements of the mesh crossed by the interface, which actually form a submesh with a band–like structure (i.e. a submesh formed by the strip of elements cut by the interface). The theoretical analysis regarding the stability of the new pressure space is not an easy task because the space depends on the arbitrary location of the interface, but it still remains possible to assess its stability by means of numerical tests. The numerical results presented in [Ausas et al. \(2010\)](#); [Sousa et al. \(2009\)](#), for (Navier–)Stokes problems exhibit good convergence properties and no spurious pressure modes, but this is far from being a rigorous numerical test. One possibility is the utilization of the patch–test ([Zienkiewicz et al., 1986](#)) or the macroelement technique ([Stenberg, 1990](#)), but the extension of these techniques considering the presence of the interface is

not trivial as mentioned. Another possibility, which is explored in this paper, is the resolution of certain eigenvalue problems (Malkus, 1981) associated to the discrete inf-sup conditions. This can be done for the two finite element discretizations considered.

The rest of the article is organized as follows: in section 2 we present the exact and discrete variational formulations for the Stokes problem, we recall the main features of the new proposed finite element space (in the two dimensional case for brevity) and we write the eigenvalue problems that are used to numerically assess the stability of both the  $P_1^+/P_1$  mini-element discretization and the equal-order  $P_1/P_1$  discretization. Section 3 shows the numerical tests performed. Finally some conclusions are drawn in section 4.

## 2 MATHEMATICAL SETTING

For simplicity we restrict ourselves to the two dimensional Stokes problem

$$-\mu \nabla^2 u + \nabla p = F_\Gamma \quad \text{in } \Omega \quad (1)$$

$$\nabla \cdot u = 0 \quad \text{in } \Omega \quad (2)$$

$$u = 0 \quad \text{on } \partial\Omega \quad (3)$$

where  $F_\Gamma = f \delta_\Gamma \mathbf{n}$ , with  $f$  a given function,  $\delta_\Gamma$  the Dirac delta distribution on the line  $\Gamma$ , and  $\mathbf{n}$  its normal. The singular force  $F_\Gamma$  acts in fact as a jump condition on the normal stress across  $\Gamma$ , namely,

$$\llbracket -p + 2\mu \frac{\partial u_n}{\partial n} \rrbracket = f, \quad (4)$$

whereas both the velocity and the tangential stress remain continuous. In fact, in this constant-viscosity case the velocity gradient exhibits no jump across  $\Gamma$  (Gross and Reusken, 2007a), so that (4) reduces to  $\llbracket p \rrbracket = -f$ .

Denoting by  $V = H_0^1(\Omega) \times H_0^1(\Omega)$ ,  $Q = L^2(\Omega)/\mathbb{R}$  and  $W = V \times Q$ , the variational formulation that corresponds to (1)-(3) reads: "Find  $(u, p) \in W$  such that

$$\int_\Omega [\mu(\nabla u + \nabla^T u) : \nabla v - p \nabla \cdot v + q \nabla \cdot u] d\Omega = \int_\Gamma f \mathbf{n} \cdot v d\Gamma \quad (5)$$

for all  $(v, q) \in W$ ". In (5) the symbol ":" stands for the double contraction of rank-two tensors. The bilinear and linear forms associated to the variational formulation are denoted by  $B(\cdot, \cdot)$  and  $L(\cdot)$ , so that (5) can be rewritten as

$$B((u, p), (v, q)) = L((v, q)). \quad (6)$$

Under reasonable regularity assumptions on  $\Gamma$  and  $f$  the linear functional  $L$  is bounded. Assuming also appropriate conditions on  $\Omega$ , and denoting by  $\phi$  and  $\psi$  the pairs  $(u, p)$  and  $(v, q)$  respectively, problem (5) is well-posed since the following known properties hold for  $B$ :

(i)

$$|B(\phi, \psi)| \leq \alpha \|\phi\|_W \|\psi\|_W \quad (7)$$

(ii)

$$\inf_{\psi \in W} \sup_{\phi \in W} \frac{B(\phi, \psi)}{\|\phi\|_W \|\psi\|_W} > 0 \quad (8)$$

with  $\alpha$  and  $\beta$  constants and  $\|\cdot\|_W$  the induced norm on  $W$  which for a function  $\phi = (u, p) \in W$  is given by

$$\|\phi\|_W^2 = \|(u, p)\|_W^2 = \|u\|_V^2 + \|p\|_Q^2 \quad (9)$$

Also, the next form of problem (5) is useful in what follows

$$a(u, v) - b(p, v) = l(v) \quad \forall v \in V \quad (10)$$

$$b(q, u) = 0 \quad \forall q \in Q \quad (11)$$

where the bilinear forms  $a(\cdot, \cdot)$  and  $b(\cdot, \cdot)$  and the linear form  $l(\cdot)$  are respectively given by

$$a(u, v) = \int_{\Omega} \mu(\nabla u + \nabla^T u) : \nabla v \, d\Omega \quad \forall v \in V \quad (12)$$

$$b(p, v) = \int_{\Omega} p \nabla \cdot v \, d\Omega \quad \forall q \in Q \quad (13)$$

$$l(v) = \int_{\Gamma} f \mathbf{n} \cdot v \, d\Gamma \quad \forall v \in V \quad (14)$$

Now, based on (12), we introduce the next equivalent norm on  $V$  to be used later on

$$\|u\|_V = \sqrt{a(v, v)} \quad \forall v \in V \quad (15)$$

## 2.1 Discrete variational formulation

This part introduces the discrete counterpart of problem (6) or of its equivalent form (10)–(11). The discrete variational formulations for both the  $P_1^+/P_1$  mini–element discretization and the equal–order  $P_1/P_1$  discretization are written. The construction of the new pressure space in the two dimensional case is then briefly recalled. Finally, we present the eigenvalue problems to numerically assess the stability of the two discretizations when the new pressure space is used instead of the standard  $P_1$  space.

### 2.1.1 Galerkin Mini–element formulation

In the Galerkin formulation, the exact variational problem is restricted to the space  $W_h = V_h \times Q_h$ , where  $V_h \subset V$  and  $Q_h \subset Q$  are the approximation spaces for velocity and pressure respectively. The discrete formulation thus reads “Find  $(u_h, p_h) \in V_h \times Q_h$  such that

$$B((u_h, p_h), (v_h, q_h)) = l(v_h) \quad (16)$$

for all  $(v_h, q_h) \in V_h \times Q_h$ ”. The mesh parameter  $h$  tends to zero as the mesh is refined.

The pressure and velocity spaces that correspond to the so-called mini–element (Arnold et al., 1984) are, for a finite element mesh  $\mathcal{T}_h$ :

$$Q_h = Q_h^1 := \{q_h \in Q \cap \mathcal{C}^0(\Omega), q_h|_K \in P_1(K), \forall K \in \mathcal{T}_h\} \quad (17)$$

$$V_h = V_h^{\text{mini}} := \{v_h \in V, v_h|_K \in (P_1(K) \oplus \text{span}(b_K))^2, \forall K \in \mathcal{T}_h\} \quad (18)$$

where  $b_K$  is the cubic bubble function that vanishes on all three edges of  $K$ . Notice that the pressure space is nothing but the usual continuous  $P_1$  space, while the space for each velocity component has been enriched by the bubble functions.

The matrix form of problem (16) is also useful for the rest of the article. Let  $\{N_a\}_{1 \leq a \leq n_u}$  be a basis for the discrete space  $V_h$  (of dimension  $n_u$ ) and  $\{M_a\}_{1 \leq a \leq n_p}$  be a basis for the discrete space  $Q_h$  (of dimension  $n_p$ ) and assume the following expansions for  $u_h$  and  $p_h$

$$u_h = \sum_{a=1}^{n_u} u_a N_a, \quad p_h = \sum_{a=1}^{n_p} p_a M_a \quad (19)$$

Now, denoting by  $\Phi = (U, P)^T = (u_1, \dots, u_{n_u}, p_1, \dots, p_{n_p})^T$ , the global column vector of nodal unknowns, problem (16) can be rewritten as

$$\begin{bmatrix} \mathbf{A} & \mathbf{B} \\ \mathbf{B}^T & \mathbf{0} \end{bmatrix} \begin{bmatrix} \mathbf{U} \\ \mathbf{P} \end{bmatrix} = \begin{bmatrix} \mathbf{F} \\ 0 \end{bmatrix} \quad (20)$$

where  $F_a = l(N_a)$ ,  $\mathbf{A} \in \mathbb{R}^{n_u \times n_u}$  and  $\mathbf{B} \in \mathbb{R}^{n_u \times n_p}$ . The element  $ab$  of these matrices is respectively given by

$$\mathbf{A}_{ab} = a(N_a, N_b) \quad (21)$$

$$\mathbf{B}_{ab} = -b(M_a, N_b) \quad (22)$$

### 2.1.2 Stabilized equal-order formulation

We are also interested in considering stabilized finite element formulations that do not satisfy the Babuška-Brezzi condition (see subsection 2.2), but are rendered convergent by means of stabilization techniques (Hughes et al., 1986; Franca and Hughes, 1988). This is the case of the equal-order  $P_1/P_1$  formulation in which the discrete spaces are

$$Q_h = Q_h^1 \quad (\text{as before}) \quad (23)$$

$$V_h = V_h^1 := \{v_h \in V, v_h|_K \in P_1(K)^2, \forall K \in \mathcal{T}_h\} \quad (24)$$

and the formulation reads: “Find  $(u_h, p_h) \in V_h \times Q_h$  such that

$$B_S((u_h, p_h), (v_h, q_h)) = l(v_h) \quad (25)$$

for all  $(v_h, q_h) \in V_h \times Q_h$ ”.

The bilinear form  $B_S$  that incorporates the stabilization is given by

$$B_S((u_h, p_h), (v_h, q_h)) = a(u_h, v_h) - b(p_h, v_h) + b(q_h, u_h) + \sum_{K \in \mathcal{T}_h} \tau_K \int_K \mathcal{R}(u_h, p_h) \cdot \nabla q_h \, dK \quad (26)$$

with the residual  $\mathcal{R}$  defined as

$$\mathcal{R}(u_h, p_h) = -\mu \nabla^2 u_h + \nabla p_h. \quad (27)$$

Note that in our case  $\nabla^2 u_h$  is identically zero since  $V_h$  consists of piecewise linear functions on  $\mathcal{T}_h$ . No analysis exists of stabilized methods in problems involving singular forces, we thus have decided to make identically zero the stabilization coefficient in the interface elements while for the rest of the elements the usual value  $h_K^2/4\mu$  is used, i.e. in our formulation the following form of coefficient  $\tau_K$  is considered

$$\tau_K = \begin{cases} h_K^2/4\mu & \text{if } K \text{ is not crossed by } \Gamma \\ 0 & \text{otherwise} \end{cases} \quad (28)$$

where  $h_K$  is the element size. It is not clear how this will affect the stability of the finite element discretization when the new pressure space (see subsection 2.3) is used. One of the objectives of the present article is precisely to investigate this.

The corresponding problem in matrix form reads

$$\begin{bmatrix} \mathbf{A} & \mathbf{B} \\ \mathbf{B}^T & \mathbf{C} \end{bmatrix} \begin{bmatrix} \mathbf{U} \\ \mathbf{P} \end{bmatrix} = \begin{bmatrix} \mathbf{F} \\ 0 \end{bmatrix} \quad (29)$$

where the matrix  $\mathbf{C}$  which incorporates the stabilization is defined as

$$\mathbf{C}_{ab} = \sum_{K \in \mathcal{T}_h} \tau_K (\nabla M_a, \nabla M_b) \quad (30)$$

Finally, as explained in [Ern and Guermond \(2004\)](#), for a function  $\phi_h \in W_h$  in this case the following norm on  $W$  should be used

$$\|\phi_h\|_W^2 = \|(u_h, p_h)\|_W^2 = \|u_h\|_V^2 + \|p_h\|_Q^2 + \sum_{K \in \mathcal{T}_h} \tau_K \|\nabla p_h\|_Q^2 \quad (31)$$

## 2.2 Stability conditions

For a given finite element formulation to be well-posed and convergent it is sufficient that the celebrated Babuška-Brezzi stability condition ([Babuška, 1973](#); [Brezzi, 1974](#)) be satisfied:

$$\inf_{q_h \in Q_h} \sup_{v_h \in V_h} \frac{b(q_h, v_h)}{\|q_h\|_Q \|v_h\|_V} \geq \gamma_0 > 0 \quad (32)$$

with  $\gamma_0$  a mesh-independent constant. This certainly holds for the case of the mini-element formulation. However, the so called LBB condition (32) is not satisfied in the case of the stabilized equal order discretization because of the choice made for  $V_h$  and  $Q_h$ . An alternative way to investigate the stability of a finite element discretization is by looking at the discrete version of the inf-sup condition (34) for the complete problem. Then, defining

$$\beta_h \doteq \inf_{(v_h, q_h) \in W_h} \sup_{(u_h, p_h) \in W_h} \frac{\mathcal{B}((u_h, p_h), (v_h, q_h))}{\|(u_h, v_h)\|_W \|(v_h, q_h)\|_W} \quad (33)$$

where the bilinear form  $\mathcal{B}(\cdot, \cdot)$  can be either  $B(\cdot, \cdot)$  defined in (5) for the mini-element discretization or  $B_S(\cdot, \cdot)$  defined in (26) for the stabilized equal-order formulation, the stability condition is that  $\exists \beta_0 > 0$  (independent of the mesh) such that

$$\beta_h \geq \beta_0 > 0 \quad (34)$$

The relevance of the inf–sup condition regarding the convergence of the finite element discretizations follows from the next inequality that can be easily proved

$$\|\phi - \phi_h\|_W \leq \left(1 + \frac{\alpha}{\beta_0}\right) \inf_{\varphi_h \in W_h} \|\phi - \varphi_h\|_W \quad (35)$$

where  $\phi = (u, p)$ ,  $\phi_h = (u_h, p_h)$  and  $\alpha$  is the constant (independent of  $h$ ) that appears in the continuity condition for  $B$  (7). Also, the “orthogonality” property of the Galerkin approximation is used in order to prove (35). To ensure solvability and optimality of the finite element solution, it is evident the importance of having the inf–sup constant  $\beta_0$  not approaching zero when the mesh size  $h$  is refined.

### 2.3 The new finite element space for discontinuous pressures

The underlying idea behind the new pressure space is to locally modify the classical conforming  $P_1$  space at those elements of  $\mathcal{T}_h$  that are cut by the interface so as to admit discontinuities at  $\Gamma$ . In the rest of the mesh the standard  $P_1$  interpolants are chosen. The new space is denoted by  $Q_h^\Gamma$ . Here, for the sake of brevity we discuss how to construct  $Q_h^\Gamma$  but restrict ourselves to the two–dimensional case. The complete description and details, for the three dimensional case, even for cases in which the interface  $\Gamma$  has an end point or a boundary inside a given element can be consulted in Ausas et al. (2010); Sousa et al. (2009).

Consider the triangle  $ABC$ , which is cut by  $\Gamma$  into subtriangle  $APQ$  and subquadrilateral  $BCQP$  (see Fig. 1). We assume for simplicity that, locally,  $\Gamma$  is approximated by linear segments. Let  $p_A, p_B, p_C$  denote the nodal values of the discrete pressure  $p_h$ , to be interpolated in the triangle  $ABC$ .

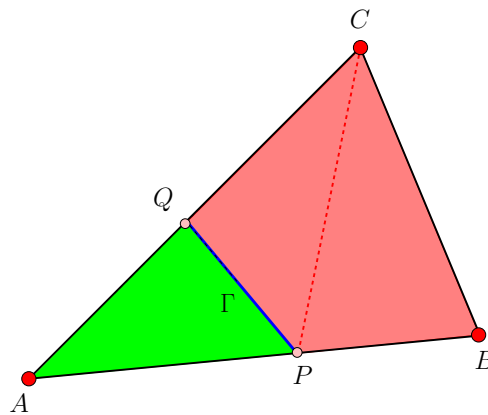


Figure 1: Partition of a single finite element into subelements following the interface  $PQ$ .

Let us arbitrarily denote the triangle  $APQ$  the “green” side of  $\Gamma$  and quadrilateral  $BCQP$  the “red” side. For the approximation to be discontinuous, the function  $p_h$  on the green side needs to be solely determined by the only green node, i.e.,  $A$ . Similarly,  $p_h$  on the red side must depend on just  $p_B$  and  $p_C$ . To accomplish this, we simply “carry” the value at each node towards the intersection of any edge emanating from it with the interface.

In this way, on the green side of  $\Gamma$ , the values at  $P$  and  $Q$  will be  $p_A$ , and thus  $p_h$  will be constant:

$$p_h|_{APQ} = p_A$$

On the red side, the value at  $P$  will be  $p_B$  and the value at  $Q$  will be  $p_C$ . One can here choose either to adopt a  $Q_1$  interpolation in  $BCQP$  from these nodal values, or subdivide the quadrilateral into two triangles,  $BCP$  and  $CQP$ . In any case, since the nodal values are given, the interpolation is immediate. For the red triangle  $CQP$ , for example,  $p_h$  will be the linear function that takes the value  $p_C$  at vertex  $C$ , the value  $p_C$  at vertex  $Q$ , and the value  $p_B$  at vertex  $P$ . Notice that this interpolation leads to  $p_h$  being discontinuous *only at*  $\Gamma$ , since the function  $p_h$  restricted to any edge of the triangle is uniquely determined by the values at the nodes lying at the endpoints of that edge.

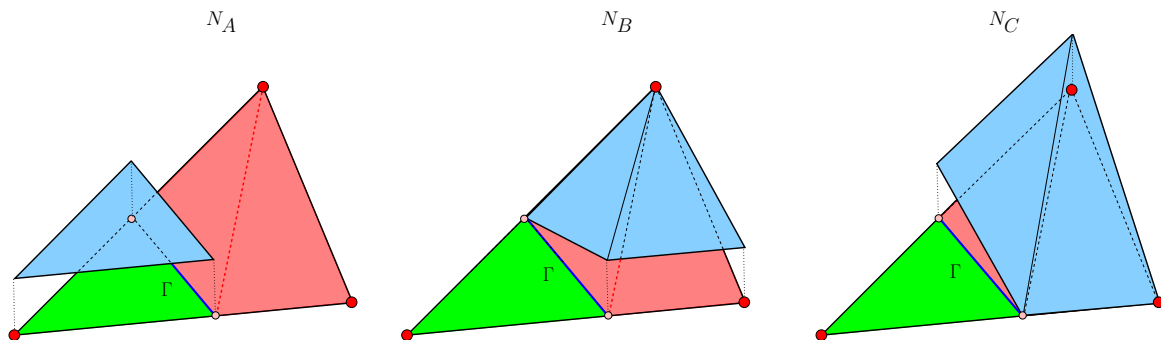


Figure 2: Basis functions for the new finite element space inside an element crossed by the interface: (a)  $N_A$ , (b)  $N_B$  and (c)  $N_C$ .

The basis functions  $N_A$ ,  $N_B$  and  $N_C$  are defined to be piecewise affine inside each of these subtriangles. It only remains to define their values at the vertices of the subtriangles, i.e., at the points  $A$ ,  $B$ ,  $C$ ,  $P$  and  $Q$ . However, since they are discontinuous at  $\Gamma$ , two values are given at points  $P$  and  $Q$ . The values on the green side will be assigned a “plus” sign, while those on the red side a “minus” sign. The values at the vertices are:

$$N_A(A) = 1 \quad N_B(A) = 0 \quad N_C(A) = 0 \quad (36)$$

$$N_A(B) = 0 \quad N_B(B) = 1 \quad N_C(B) = 0 \quad (37)$$

$$N_A(C) = 0 \quad N_B(C) = 0 \quad N_C(C) = 1 \quad (38)$$

$$N_A(P^+) = 1 \quad N_B(P^+) = 0 \quad N_C(P^+) = 0 \quad (39)$$

$$N_A(P^-) = 0 \quad N_B(P^-) = 1 \quad N_C(P^-) = 0 \quad (40)$$

$$N_A(Q^+) = 1 \quad N_B(Q^+) = 0 \quad N_C(Q^+) = 0 \quad (41)$$

$$N_A(Q^-) = 0 \quad N_B(Q^-) = 0 \quad N_C(Q^-) = 1 \quad (42)$$

This new finite element space is much easier to implement than the one proposed by [Gross and Reusken \(2007a\)](#), which is based on the XFEM enrichment, and also than the one proposed by [Fries and Belytschko \(2006\)](#), which avoids introducing additional unknowns by switching to a moving-least-squares approximation in the vicinity of  $\Gamma$ . The interpolation properties of the new space are shown numerically in [Ausas et al. \(2010\)](#) by means of several numerical tests, including problems with imposed singular forces and problems including surface tension effects, both in 2D and 3D. Also a theoretical proof of convergence has been presented in [Buscaglia and Agouzal \(2009\)](#). Briefly, the interpolation accuracy of the proposed space is  $\mathcal{O}(h^{\frac{3}{2}})$  in the  $L^2(\Omega)$ -norm, which is suboptimal for piecewise linear elements. However,  $Q_h^\Gamma$  does not limit the accuracy of a (Navier-)Stokes calculation neither in equal-order velocity-

pressure approximations, nor in the mini–element approximation for which the global accuracy is limited by the  $H^1(\Omega)$ –accuracy of the velocity space, which is  $\mathcal{O}(h)$ .

## 2.4 The eigenvalue problems

The aim in this paper is to study the stability of both discretizations presented in section 2.1 when the new pressure space  $Q_h^\Gamma$  is used in the place of  $Q_h^1$  in (17) and (23). This study is conducted by means of solving different eigenvalue problems. The first eigenvalue problem gives the natural modes for the Stokes problem, the second eigenvalue problem is associated to the discrete inf–sup condition (including the complete bilinear form) and finally, the last problem is connected to the well known LBB condition. We briefly recall these problems in what follows. For all the details, in particular their eigenstructure and connection among them the reader is referred to Malkus (1981).

### 2.4.1 Natural modes eigenproblem

The first eigenproblem that can bring insight on the stability of the finite element discretizations previously described when the new pressure space is used, is the problem to compute the natural eigenmodes associated to the Stokes operator. In principle, the problem to be solved is: Find eigenvalues  $\lambda \in \mathbb{R}$  and non–zero eigenfunctions  $u \in V_{\text{div}}$  such that

$$-\mu \nabla^2 u = \lambda u \quad \text{in } \Omega \tag{43}$$

$$u = 0 \quad \text{on } \partial \Omega \tag{44}$$

where  $V_{\text{div}}$  is the space of solenoidal vector fields. This problem is equivalent to the following one: Find  $(\lambda, u) \in \mathbb{R} \times V$  that satisfy

$$-\mu \nabla^2 u + \nabla p = \lambda u \quad \text{in } \Omega \tag{45}$$

$$\nabla \cdot u = 0 \quad \text{in } \Omega \tag{46}$$

$$u = 0 \quad \text{on } \partial \Omega \tag{47}$$

The discrete weak form of this problem reads: “Find  $(\lambda_h, u_h) \in \mathbb{R} \times V_h$  such that

$$\mathcal{B}((u_h, p_h), (v_h, q_h)) = \lambda_h (u_h, v_h) \tag{48}$$

for all  $(v_h, q_h) \in V_h \times Q_h$ ”, where again  $\mathcal{B}(\cdot, \cdot)$  can be either  $B(\cdot, \cdot)$  or  $B_S(\cdot, \cdot)$  and

$$(u_h, v_h) = \int_{\Omega} u_h \cdot v_h \, d\Omega \tag{49}$$

is the  $L^2(\Omega)$  inner product. Problem (48) can be written in matrix form as follows

$$\begin{bmatrix} \mathbf{A} & \mathbf{B} \\ \mathbf{B}^T & \mathbf{E} \end{bmatrix} \begin{bmatrix} \mathbf{U} \\ \mathbf{P} \end{bmatrix} = \lambda \begin{bmatrix} \mathbf{M} & \mathbf{0} \\ \mathbf{0} & \mathbf{0} \end{bmatrix} \begin{bmatrix} \mathbf{U} \\ \mathbf{P} \end{bmatrix} \tag{50}$$

where matrices  $\mathbf{A}$  and  $\mathbf{B}$  were defined in (21) and (22) respectively. The matrix  $\mathbf{E} \in \mathbb{R}^{n_p \times n_p}$  is identically  $\mathbf{0}$  for the mini–element discretization while for the stabilized equal–order discretization corresponds to the matrix  $\mathbf{C}$ . The block matrix appearing in the left hand side of (50) will

be denoted with the symbol  $\mathbf{K}$  later. The velocity “mass” matrix  $\mathbf{M} \in \mathbb{R}^{n_u \times n_u}$  appearing in the right hand side is simply defined as

$$\mathbf{M}_{ab} = (N_a, N_b) \quad (51)$$

*Remark:* It should be noted that the matrix appearing in the right hand side of (50) is singular which leads to an ill-posed system as discussed in Moler and Stewart (1973).

It can be proved that for each  $m \in \mathbb{N}$  and for the mesh parameter  $h$  sufficiently small, the exact  $(\mu_m, (u, p)_m) \in \mathbb{R} \times W$  eigenpair and its discrete counterpart  $(\mu_{h,m}, (u_h, p_h)_m) \in \mathbb{R} \times W_h$  satisfy the following error estimates (Babuška and Osborn, 1991).

$$\mu_m \leq \mu_{h,m} \leq (1 + c h^{2p})\mu_m, \quad \|(u, p)_m - (u_h, p_h)_m\|_W \leq C(m)h^p \quad (52)$$

where  $p = 1$  in our case since we are using linear elements and the constants  $c$  and  $C(m)$  are independent of the mesh.

In order to study the convergence of the finite element solution, the inf-sup condition for the complete problem (34) or the LBB condition (32) have to be verified. These two conditions lead to different eigenvalue problems which are presented in the two following subsections.

#### 2.4.2 Inf-Sup eigenproblem

First, considering (9) and (15), the norm on  $W$  in matrix form reads

$$\|(u_h, p_h)\|_W^2 = \Phi^T \mathbf{N} \Phi = \mathbf{U}^T \mathbf{A} \mathbf{U} + \mathbf{P}^T \mathbf{Q} \mathbf{P} \quad (53)$$

where the matrix  $\mathbf{N}$  is defined as

$$\mathbf{N} = \begin{bmatrix} \mathbf{A} & \mathbf{0} \\ \mathbf{0} & \mathbf{Q} \end{bmatrix} \quad (54)$$

and where the pressure mass matrix  $\mathbf{Q} \in \mathbb{R}^{n_p \times n_p}$  for the case of the mini-element discretization is just defined as

$$\mathbf{Q}_{ab} = (M_a, M_b) \quad (55)$$

For the stabilized equal-order discretization, the matrix  $\mathbf{Q}$  must also include the contribution of the stabilization (i.e. matrix  $\mathbf{C}$  defined in equation (30) has to be added). In this case, considering the following quotient

$$R(\Phi, \Psi) = \frac{\Phi^T \mathbf{K} \Psi}{(\Phi^T \mathbf{N} \Phi)^{\frac{1}{2}} (\Psi^T \mathbf{N} \Psi)^{\frac{1}{2}}} \quad (56)$$

it can be shown that the inf-sup value of (56) is the smallest (in magnitude) non-zero eigenvalue of the following generalized eigenvalue problem

$$\mathbf{K} \Phi = \lambda \mathbf{N} \Phi \quad (57)$$

and actually gives the inf–sup constant  $\beta_0$  (Malkus, 1981). Also the number of zero eigenvalues indicates the number of pressure modes (be it constant modes or spurious pressure modes).

*Remark:* We observe that the eigenvalues for this problem are in  $\{\mathbb{R} \setminus (0, 1)\}$ . This can be easily seen by eliminating  $P$  from the system (57) i.e.,

$$\mathbf{BQ}^{-1}\mathbf{B}^T\mathbf{U} = (\lambda^2 - \lambda)\mathbf{AU} \quad (58)$$

after premultiplication by  $\mathbf{U}^T$  to both sides we obtain

$$(\mathbf{B}^T\mathbf{U})^T\mathbf{Q}^{-1}(\mathbf{B}^T\mathbf{U}) = (\lambda^2 - \lambda)(\mathbf{U}^T\mathbf{AU}) \quad (59)$$

Now, noting that the left hand side and the factor  $\mathbf{U}^T\mathbf{AU}$  are both positive, it follows that  $\lambda^2 - \lambda > 0$ . Hence, the initial observation follows.

### 2.4.3 LBB eigenproblem

Another eigenvalue problem is the one associated to the discrete LBB condition (32). The corresponding problem in matrix form reads

$$\mathbf{GU} = \lambda\mathbf{AU} \quad (60)$$

where the matrix  $\mathbf{G}$  is given by

$$\mathbf{G} = \mathbf{BQ}^{-1}\mathbf{B}^T \quad (61)$$

It can be proved that the inf–sup value of the following expression

$$g(\mathbf{U}, \mathbf{P}) = \frac{\mathbf{U}^T\mathbf{BP}}{(\mathbf{U}^T\mathbf{AU})^{\frac{1}{2}}(\mathbf{P}^T\mathbf{QP})^{\frac{1}{2}}} \quad (62)$$

is given by the square root of the smallest non–zero eigenvalue of the generalized problem (60). This problem is solved for instance in Chapelle and Bathe (1993); Bathe (2001) to study the stability of several finite element pairs. For the case of the stabilized formulation, certainly the discrete LBB condition is not satisfied. For the case of the stable mini–element, there is an equivalence between the inf–sup and LBB eigenproblems (see Babuška et al. (1977); Brezzi (1974)), for which reason we restrict our attention to the first two eigenvalue problems.

## 3 NUMERICAL RESULTS

### 3.1 Natural modes

Before proceeding to the numerical results a few comments should be made regarding the resolution of the eigenvalue problems in this paper: on the one hand, for those tests considering the stabilized equal–order discretization we use the SLEPc routines (Scalable Library for Eigenvalue Problem Computations (Fernández et al., 2003)) with their default solver based on a Krylov–Schur method. On the other hand, for those cases using the mini–element discretization we use the default solver provided in the MATLAB software, which are based on the ARPACK library, implementing the Arnoldi/Lanczos method (Lehoucq and Sorensen, 1996; Lehoucq et al., 1998). The homogeneous Dirichlet boundary conditions are dealt by means of replacing the corresponding rows and columns in the system matrices with vectors containing zero entries at all positions except at the one corresponding to the diagonal where an arbitrary value of 1000

and 1 are placed on the left and right hand side matrices respectively. In this way we are able to shift these eigenvalues (all equal to 1000) that are unimportant to us. A careful analysis of the eigenmodes for the Stokes operator in square domains have been carried out in [Leriche and Labrosse \(2004\)](#); [Leriche et al. \(2008\)](#) by means of a pseudo-spectral solver in primitive variables and also by means of a Galerkin-Reid-Harris expansion for the stream function. In this part we use their results to compare with our numerically computed eigenvalues. The natural eigenmodes are calculated on the computational domain  $\Omega = [-1, 1] \times [-1, 1]$ . The domain is discretized with an unstructured mesh consisting of 208 triangular elements (shown in figure 3) to which we assign a mesh size of  $h = 0.222$ . A sequence of meshes is built by successively dividing each of the triangles of the previous mesh into four equal triangles leading to meshes with  $h = 0.111$ ,  $h = 0.0555$  and so forth, until the finest mesh with  $h = 3.468 \times 10^{-3}$  (with 851968 elements).

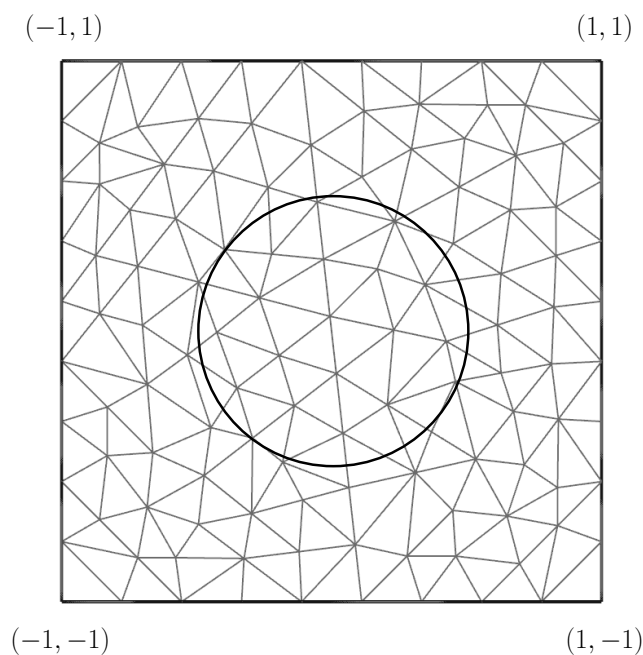


Figure 3: First mesh of the sequence used to numerically assess the stability of the finite element discretizations with the new pressure space  $Q_h^\Gamma$ .

For the cases considered in this paper the interface is fixed. Considering an arbitrary triangulation  $\mathcal{T}_h$  we define a continuous scalar function  $\phi_h$  whose zero level set represents the interface  $\Gamma_h$ , i.e.

$$\Gamma_h = \{ \mathbf{x} \in \mathbb{R}^2, \phi_h(\mathbf{x}) = 0 \}. \quad (63)$$

The function  $\phi_h$  is linearly approximated on each triangle  $K \in \mathcal{T}_h$  such that  $\Gamma_h$  is made up of linear segments. In the first place, in figure 4 we show a few eigenmodes. In this case we use the space  $Q_h^\Gamma$  and the stabilized equal order finite element discretization (results shown in the figure correspond to the third level of refinement). The interface in this case consists of a circle of radius 0.5 centered at the origin. The presence of the interface should obviously not affect the eigenmodes, being just in this case “an excuse” to use the new pressure space  $Q_h^\Gamma$ . Actually, almost the same results are observed when the usual  $Q_h^1$  is used instead. Table 1 shows the numerically computed eigenvalues for the sequence of meshes considered and compare

them with the best computed values presented in [Leriche and Labrosse \(2004\)](#) denoted by  $\lambda_L$ . Comparison is made just with the eigenvalues of the so called first family, which corresponds to a given symmetry of the eigenmodes, although the authors also report the corresponding values for other symmetry families. Figure 5 shows the error for the fundamental mode as a function of the mesh size  $h$  indicating the expected quadratic convergence according to equation (52). The numerical results are very similar when the usual space  $Q_h^1$  is used. These results already show that the presence of the new pressure space  $Q_h^\Gamma$  does not affect the expected convergence rate for the eigenvalues. Computations performed with the stable mini–element, with and without the pressure space  $Q_h^\Gamma$  have shown similar results, that are not reported here for brevity.

Table 1: The fourth fundamental numerically computed eigenvalues for the different meshes. Comparison is made with the values computed in [Leriche and Labrosse \(2004\)](#).

$h$	$\lambda_1$	$\lambda_2$	$\lambda_3$	$\lambda_4$
$2.222 \times 10^{-1}$	13.798805073	44.225211341	78.212853652	89.159923572
$1.111 \times 10^{-1}$	13.271513867	40.057026489	65.936555818	89.332331324
$5.555 \times 10^{-2}$	13.133488239	42.211293398	62.694812557	89.316161415
$2.777 \times 10^{-2}$	13.098078584	41.871367662	61.861870158	91.249430127
$1.388 \times 10^{-2}$	13.089150758	41.785839139	61.651812681	90.828313457
$6.944 \times 10^{-3}$	13.086916811	41.764428684	61.599262202	90.722918673
$3.472 \times 10^{-3}$	13.086358678	41.759077002	61.586154019	90.696567988
<i>Leriche et al</i>	13.086172791	41.757293817	61.581799188	90.687786716

### 3.2 Complete Inf–Sup eigenproblem

This part presents the results corresponding to the resolution of the generalized eigenvalue problem (57) associated to the inf–sup condition for the complete bilinear form. This is used to evaluate the stability of the new pressure space embedded in the the equal–order discretization and the stable mini–element.

The interface  $\Gamma_h$  that is considered in this case is shown in figure 6. It corresponds to four random bubbles placed again in the square domain  $\Omega = [-1, 1] \times [-1, 1]$ . These are generated with the only requirement that the smallest distance between them be greater than three times the typical element size  $h_K$ . This is needed to avoid the complete lack of stabilization which typically occurs when in all the elements that share a given node of the mesh the stabilization constant  $\tau_K$  is set to zero as explained in section (2.1.2). The idea of choosing this random pattern is to consider, in some way, a more general interface with which to test the new pressure space  $Q_h^\Gamma$ , i.e. to consider more possible forms in which the interface cut the elements of the mesh. Independence of results with respect to this random interface was verified, however, a more rigorously statistical study is the subject of ongoing work. In this form we consider more possible ways in which the interface cuts the elements of the mesh.

The same routines previously mentioned are used in this case to solve the eigenvalue problem. In Table 2 and 3 we report the numerically computed eigenvalues for the generalized problem (57) for the same sequence of meshes previously considered. First, in table 2 we observe an eigenvalue which is essentially zero. This first eigenvalue corresponds to the constant pressure mode. Then, we observe a series of eigenvalues different from zero. Remember that the smallest non–zero eigenvalue of the generalized problem (57) gives the inf–sup constant  $\beta_0$  which we aim to evaluate here. An eigenvalue approaching zero as the mesh is refined would

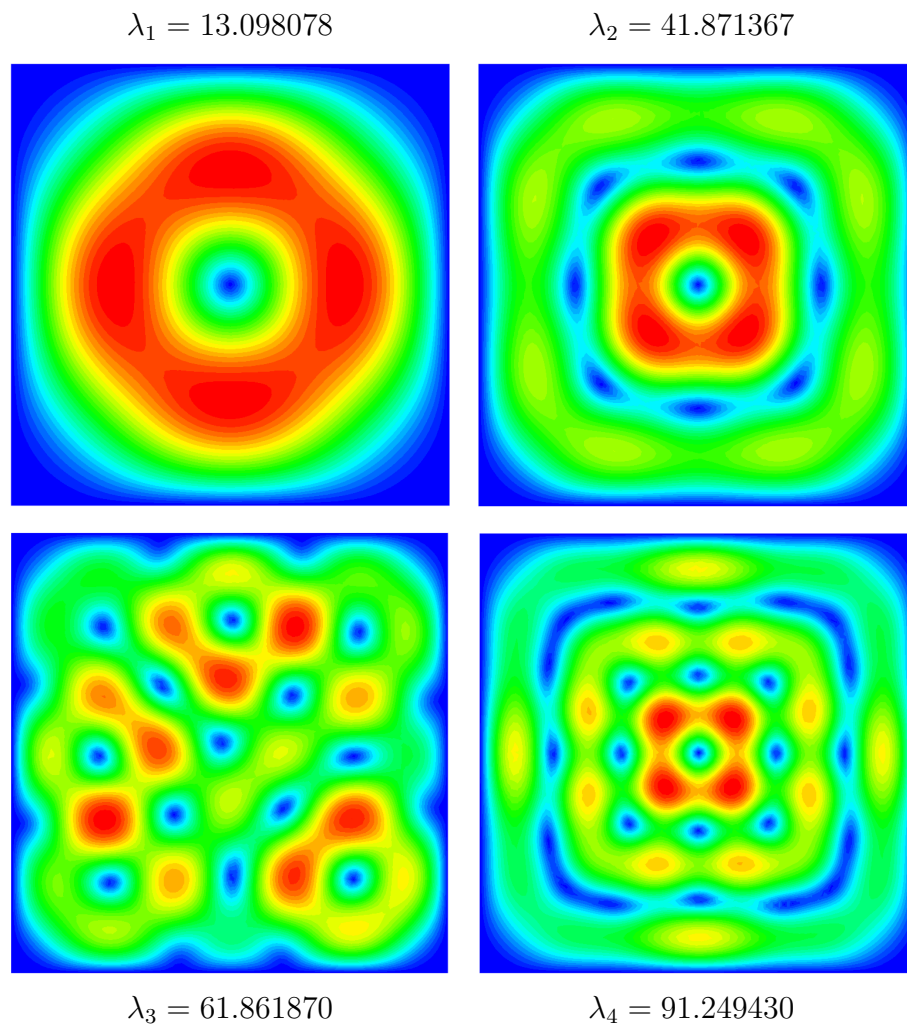


Figure 4: Velocity magnitude for the first eigenmodes obtained by means of the stabilized equal-order discretization with the new pressure space  $Q_h^F$  in the presence of a circular interface. Results corresponds to the third level of refinement ( $h = 2.777 \times 10^{-2}$ ).

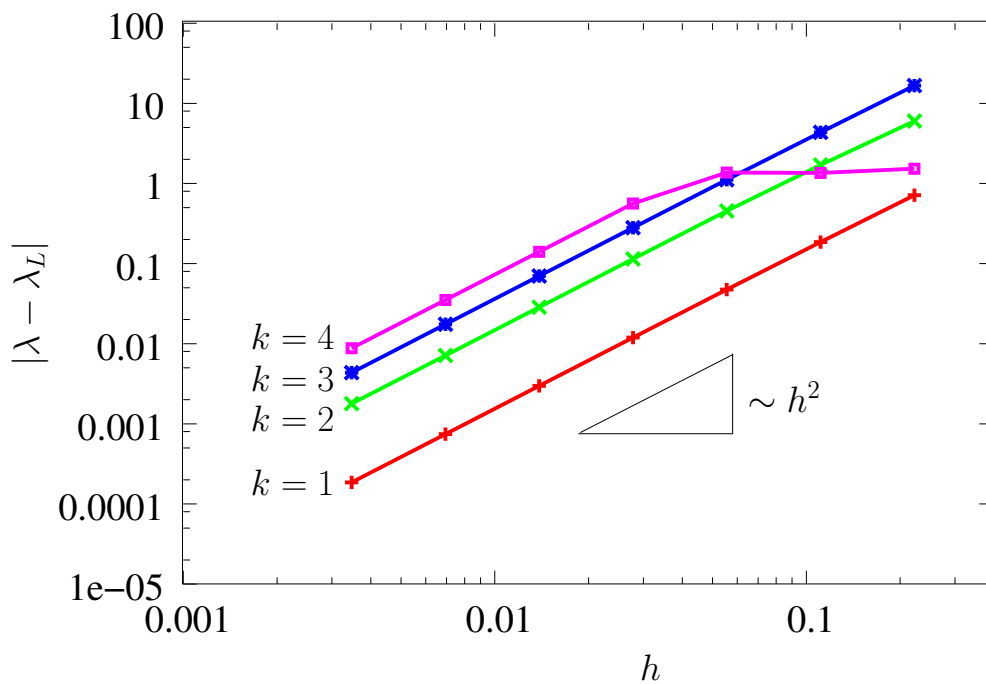


Figure 5: Eigenvalues error  $|\lambda - \lambda_L|$  as a function of the mesh size  $h$  for the eigenmodes shown in figure 4.

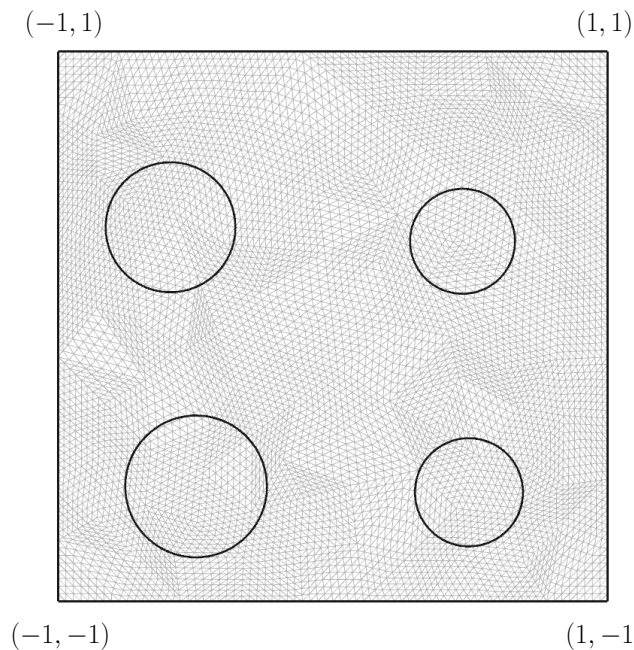


Figure 6: Interface with which the new pressure space is  $Q_h^\Gamma$  is tested. Also shown the underlying mesh corresponding to the third level of refinement ( $h = 2.777 \times 10^{-2}$ ).

indicate the presence of spurious pressure modes. The table shows that the inf-sup value  $\lambda_2$  approaches a constant value approximately equal to 0.146. Note that for the last mesh (sixth level of refinement consisting of  $\sim 851000$  elements) the eigenvalue just reduced to the  $\sim 85\%$  of its value corresponding to the first mesh of the sequence (with 208 elements) Also interesting in this case are the eigenmodes. In figure 7 we show their corresponding velocity contours. No

evidence of spurious modes is observed. Note also that the eigenmodes 3 and 4 are the same (up to a rotation) and actually the eigenvalues  $\lambda_3$  and  $\lambda_4$  converge to the same value as the mesh is refined (as seen in table 2), i.e. this is an eigenvalue of multiplicity 2. On the other hand, when the stabilization is removed all over the mesh the spurious modes clearly show up as observed in figure 8 where two different eigenmodes are shown. Note the typical chess board pattern of the pressure field (top). Also shown are the contours of the velocity magnitude (bottom).

Table 2: First numerically computed eigenvalues for problem (57) for the stabilized equal-order formulation with the new pressure space.

$h$	$\lambda_1$	$\lambda_2$	$\lambda_3$	$\lambda_4$	$\lambda_5$	$\lambda_6$
$2.222 \times 10^{-1}$	$7.2 \times 10^{-11}$	0.1735459	0.1786114	0.1833031	0.2086292	0.2151264
$1.111 \times 10^{-1}$	$3.4 \times 10^{-11}$	0.1693879	0.1711110	0.1715619	0.1924594	0.2469373
$5.555 \times 10^{-2}$	$2.5 \times 10^{-11}$	0.1619650	0.1629666	0.1630474	0.1766542	0.2244143
$2.777 \times 10^{-2}$	$2.7 \times 10^{-11}$	0.1560775	0.1567810	0.1567900	0.1658042	0.2060746
$1.388 \times 10^{-2}$	$2.0 \times 10^{-12}$	0.1519014	0.1524095	0.1524105	0.1586891	0.1930118
$6.944 \times 10^{-3}$	$9.9 \times 10^{-11}$	0.1489017	0.1492813	0.1492813	0.1538491	0.1833692
$3.472 \times 10^{-3}$	$1.2 \times 10^{-10}$	0.1466543	0.1469451	0.1469451	0.1503730	0.1759538

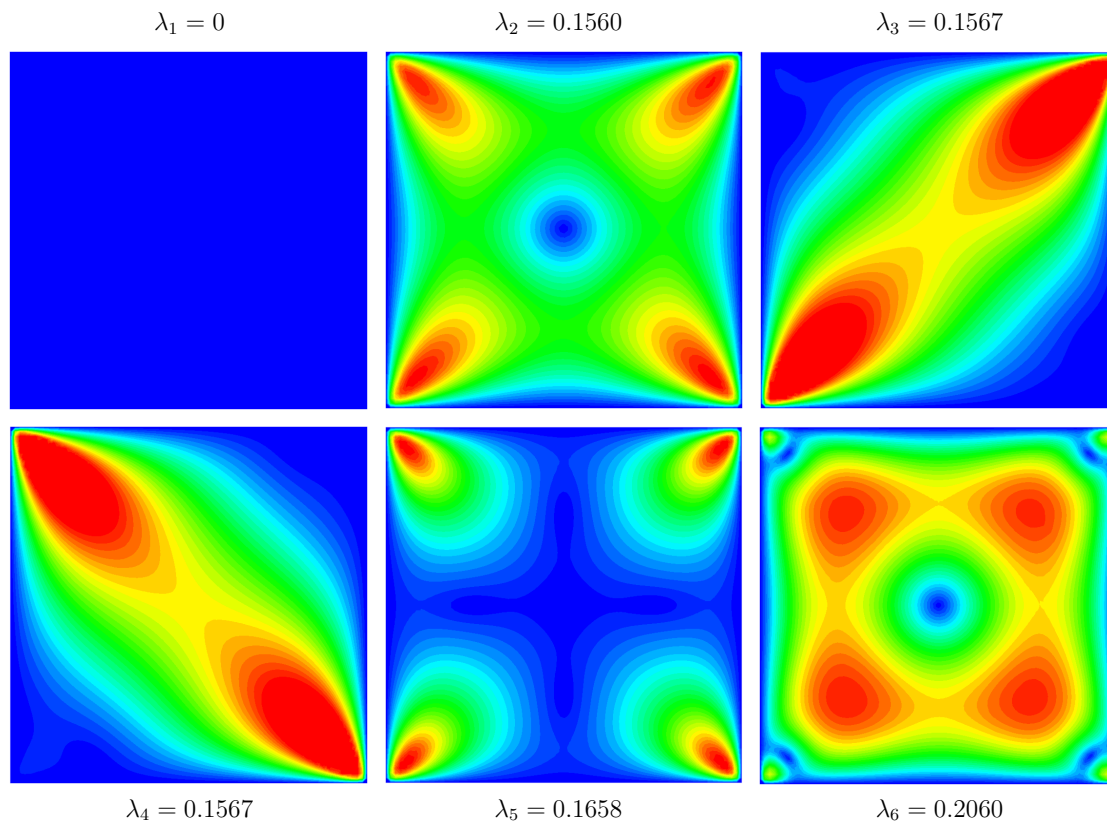


Figure 7: Velocity magnitude for the first eigenmodes of problem (57) obtained by means of the stabilized equal-order discretization with the new pressure space  $Q_h^\Gamma$  in the presence of the three random bubbles. Results correspond to the third level of refinement ( $h = 2.777 \times 10^{-2}$ ).

In Table 3 are reported the first computed eigenvalues for the stable mini-element with  $Q_h^\Gamma$ , showing almost the same behavior as the stabilized formulation. In this case however, it can be

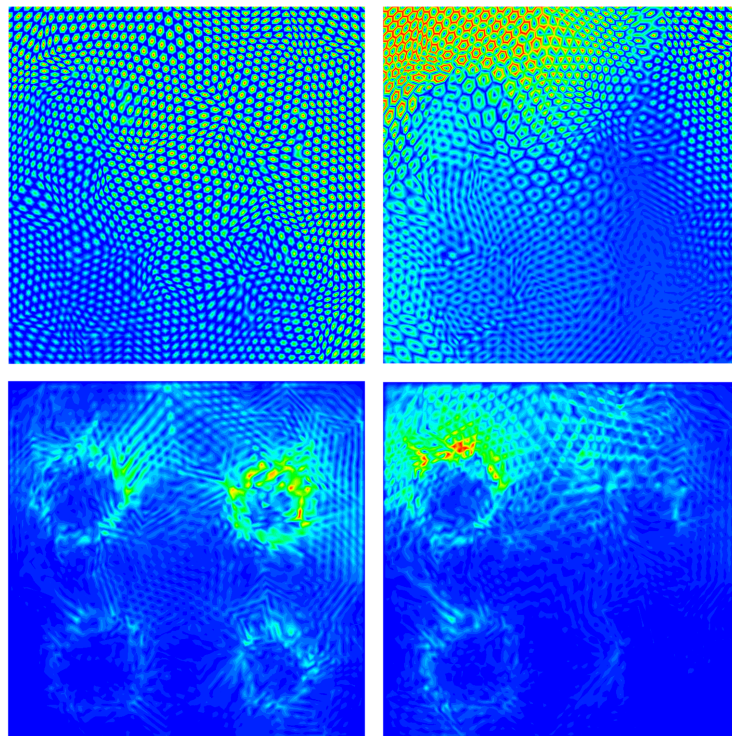


Figure 8: Spurious modes appearing when the stabilization is completely removed. Shown are contours of pressure (top) and the velocity magnitude (bottom). Results corresponds to the third level of refinement.

seen that the first non-zero eigenvalue  $\lambda_2$ , which is the inf-sup value, increases its magnitude as meshes are refined.

The numerically computed inf-sup constant  $\beta_0$  shows that the new pressure space does not introduce any spurious modes in both stable and stabilized formulations.

Table 3: First numerically computed eigenvalues for problem (57) for the  $P_1^+/P_1$  discretization with the new pressure space.

$h$	$\lambda_1$	$\lambda_2$	$\lambda_3$	$\lambda_4$	$\lambda_5$	$\lambda_6$
$2.222 \times 10^{-1}$	$2.6 \times 10^{-15}$	0.0537786	0.0538273	0.0538375	0.0554217	0.1065293
$1.111 \times 10^{-1}$	$1.3 \times 10^{-15}$	0.0554078	0.0555215	0.0555274	0.0560010	0.0965297
$5.555 \times 10^{-2}$	$8.8 \times 10^{-16}$	0.0557147	0.0557265	0.0557283	0.0558794	0.0851426
$2.777 \times 10^{-2}$	$2.8 \times 10^{-16}$	0.0557154	0.0557163	0.0557165	0.0557638	0.0744133
$1.388 \times 10^{-2}$	$1.2 \times 10^{-16}$	0.0557125	0.0557128	0.0557128	0.0557273	0.0679186

## 4 CONCLUSIONS

The numerical stability of a new pressure space with embedded discontinuities for two different finite element discretizations of the Stokes problem was investigated by means of numerically solving three different eigenvalue problems: on the one hand, the natural eigenmodes of the Stokes problem and on the other hand, a problem associated to the discrete inf-sup condition. The two discretizations considered are the  $P_1^+/P_1$  mini-element and the equal-order  $P_1/P_1$  stabilized formulation.

For the first eigenproblem, the numerical results showed that the presence of the new pressure space does not affect the expected convergence rate of the eigenvalues. In this case an interface formed by a single circular bubble was considered to justify the use of the new pressure space. In the second case, corresponding to the inf–sup condition for the complete bilinear form it was considered an interface formed by four random circular bubbles so as to cover more possible ways in which the interface cuts the elements of the partition. The computed inf–sup constant, for both discretizations, does not approaches zero under mesh refinement.

This stability analysis jointly with the interpolation properties numerically shown in Ausas et al. (2010) and theoretically in Buscaglia and Agouzal (2009) demonstrate that the numerical formulation with the new propose pressure space is convergent.

### ACKNOWLEDGMENTS

The authors acknowledge partial support from FAPESP (Brazil), CNPq (Brazil), CNEA (Argentina) and CONICET (Argentina). This research was carried out in the framework of INCT-MACC, Ministério de Ciência e Tecnologia, Brazil.

### REFERENCES

- Arnold D., Brezzi F., and Fortin M. A stable finite element for the Stokes equations. *Calcolo*, 21:337–344, 1984.
- Ausas R., Sousa F., and Buscaglia G. An improved finite element space for discontinuous pressures. *Comput. Methods Appl. Mech. Engrg.*, 199:1019–1031, 2010.
- Babuška I. The finite element method with Lagrangian multipliers. *Numer. Math.*, 20:179–192, 1973.
- Babuška I., Oden J.T., and Lee J. Mixed–hybrid finite element approximations of second order elliptic boundary value problems. *Comput. Methods Appl. Mech. Engrg.*, 11:175–206, 1977.
- Babuška I. and Osborn J. *Eigenvalue Problems, in Handbook of Numerical Analysis, eds. P. G. Ciarlet and J. L. Lions*, volume II. North Holland, 1991.
- Bathe K. The inf–sup condition and its evaluation for mixed finite element methods. *Computers and Structures*, 79:243–252, 2001.
- Belytschko T., Moës N., Usui S., and Parimi C. Arbitrary discontinuities in finite elements. *Int. J. Numer. Meth. Engng*, 50:993–1013, 2001.
- Brezzi F. On the existence, uniqueness and approximation of saddle–point problems arising from Lagrange multipliers. *RAIRO Anal. Numér.*, 8:129–151, 1974.
- Buscaglia G. and Agouzal A. Interpolation estimate for a finite element space with embedded discontinuities. *Proc. 30th Iberian-Latin-American Congress on Computational Methods in Engineering, Búzios, Brazil, November 8–11, 2009*.
- Chapelle D. and Bathe K. The inf–sup test. *Computers and Structures*, 47:537–545, 1993.
- Ern A. and Guermond J.L. *Theory and Practice of Finite Elements*. Springer, 2004.
- Fernández V., Román J., and Vidal V. SLEPc: Scalable library for eigenvalue problem computations. *Lecture Notes in Computer Science*, 2565:377–391, 2003.
- Franca L. and Hughes T. Two classes of mixed finite element methods. *Comput. Methods Appl. Mech. Engrg.*, 69:89–129, 1988.
- Fries T.P. and Belytschko T. The intrinsic XFEM: a method for arbitrary discontinuities without additional unknowns. *Int. J. Numer. Meth. Engng.*, 68:1358–1385, 2006.
- Gross S. and Reusken A. An extended pressure finite element space for two-phase incompressible flows with surface tension. *J. Comput. Phys.*, 224:40–58, 2007a.

- Gross S. and Reusken A. Finite element discretization error analysis of a surface tension force in two-phase incompressible flows. *SIAM J. Numer. Anal.*, 45:1679–1700, 2007b.
- Hughes T., Franca L., and Balestra M. A new finite element formulation for computational fluid dynamics: V. circumventing the babuška-brezzi condition. a stable petrov-galerkin formulation of the Stokes problem accommodating equal-order interpolations. *Comput. Methods Appl. Mech. Engrg.*, 59:85–99, 1986.
- Lehoucq R. and Sorensen D. Deflation techniques for an implicitly re-started Arnoldi iteration. *SIAM J. Matrix Analysis and Applications*, 17:789–821, 1996.
- Lehoucq R., Sorensen D., and Yang C. *ARPACK Users' Guide: Solution of Large-Scale Eigenvalue Problems with Implicitly Restarted Arnoldi Methods*. SIAM Publications, 1998.
- Leriche E. and Labrosse G. Stokes eigenmodes in square domain and the stream function–vorticity correlation. *J. Comput. Phys.*, 200:489–511, 2004.
- Leriche E., Lallemand P., and Labrosse G. Stokes eigenmodes in cubic domain: primitive variable and lattice boltzmann formulations. *App. Numer. Math.*, 58:935–945, 2008.
- Malkus D. Eigenproblems associated with the discrete LBB condition for incompressible finite elements. *Int. J. Engng. Sci.*, 19:1299–1310, 1981.
- Minev P., Chen T., and Nandakumar K. A finite element technique for multifluid incompressible flow using Eulerian grids. *J. Comput. Phys.*, 187:225–273, 2003.
- Moler C. and Stewart G. An algorithm for generalized matrix eigenvalue problems. *SIAM J. Numer. Anal.*, 10(2):241–256, 1973.
- Reusken A. Analysis of an extended pressure finite element space for two–phase incompressible flows. *Comput. Visual. Sci.*, 11:293–305, 2008.
- Sousa F., Ausas R., and Buscaglia G. Improved interpolants for discontinuous pressures. *Serie Mecánica Computacional*, XXVIII:1131–1148, 2009.
- Stenberg R. A technique for analysing finite element methods for viscous incompressible flow. *Int. J. Num. Meth. in Fluids*, 11:935–948, 1990.
- Zienkiewicz O., Qu S., Taylor R., and Nakazaw S. The patch test for mixed formulations. *Int. J. Num; Meth. Engng.*, 23:1873–1883, 1986.